

THIS IS A PREPRINT --- SUBJECT TO CORRECTION

Simulation of Heat Flow in Porous Media Using Numerical Models

By

F. R. Nicholson, Member AIME, W. W. Jones and Klaus Schwabe, Jr. Member, AIME,
D. R. McCord and Associates, Inc., Dallas, Tex.

© Copyright 1968

American Institute of Mining, Metallurgical and Petroleum Engineers, Inc.

This paper was prepared for the SPE European Regional Meeting, to be held in Milano, Italy, April 4-7, 1968. Permission to copy is restricted to an abstract of not more than 300 words. Illustrations may not be copied. The abstract should contain conspicuous acknowledgment of where and by whom the paper is presented. Publication elsewhere after publication in the JOURNAL OF PETROLEUM TECHNOLOGY or the SOCIETY OF PETROLEUM ENGINEERS JOURNAL is usually granted upon request to the Editor of the appropriate journal provided agreement to give proper credit is made.

Discussion of this paper is invited. Three copies of any discussion should be sent to the Society of Petroleum Engineers office. Such discussion may be presented at the above meeting and, with the paper, may be considered for publication in one of the two SPE magazines.

ABSTRACT

Generalized heat and fluid flow models are useful in evaluating the effects of heat upon crude oils in a reservoir environment and more particularly that area immediately surrounding a wellbore. The model described allows fluid and heat flow in the two dimensions of a vertical plane. As in other numerical models, each cell is assumed to be homogeneous in pressure, viscosity, temperature, etc. This paper describes how the flow of heat from one cell to another has been superimposed upon the unsteady-state flow of oil, gas, water, and steam between cells. Solutions to problems using this reservoir simulator are shown.

INTRODUCTION

During the last several years the use of numerical models to simulate reservoir conditions have become very commonplace and simulators of several types and configurations have been developed for solution on high speed digital computers. During these same years, thermal recovery techniques have received a great deal of attention, and numerical simulator solutions applied also to this area. The broad term of thermal recovery covers a spectrum from in situ combustion to hot water alteration of fluid saturations around wellbores. Thermal recovery, like many other popular techniques, has a

certain amount of "romance" surrounding it. The benefits can be very substantial; however, like any new technique it is subject to misapplication. The purpose of this paper is to describe a numerical simulator that accounts for both fluid and heat flow, and further to relate some of the observations that have evolved from its use.

DISCUSSION OF THE THERMAL MODEL

The concept used in designing this thermal model was to combine fluid and heat flow into one model. The continuity equations written for each mobile phase (oil, gas, and water) were summed employing the method proposed by Fagin et al¹. The equations were arranged for an implicit solution of the potential distributions using the alternating direction procedure of Peaceman and Rachford². Following the calculation of the potential distributions, the saturation distribution and temperature distribution are calculated explicitly. An iterative procedure of the entire calculation sequence permits the use of conductance and expansion coefficients calculated forward in time. This forward approximation is particularly important in the model discussed here because expansion and phase changes are not only functions of pressure but also of temperature. This approach permitted the use of relatively long time increments which are essential for the use of the simulator in the solution of practical engineering problems.

References and illustrations at end of paper.

The equation of state for each mobile phase, Darcy's flow formula, the conservation of mass and heat energy were combined to develop a set of mathematical equations which may be solved by large scale digital computers within an economical length of time. Differential equations describing fluid flow, considering x and y as the Cartesian coordinates in a two-dimensional system (see Figure 1), are as follows:

For gas:

$$\begin{aligned} \nabla \cdot \left[\left(\frac{kh}{B\mu} \right)_g \nabla \Phi_g \right] - \nabla \cdot \left[R_L \left(\frac{kh}{B\mu} \right)_o \nabla \Phi_o \right] \\ = \frac{\partial}{\partial t} \left(\phi h \frac{S_g}{B_g} \right) - \frac{\partial}{\partial t} \left(\frac{\phi h R_L S_o}{B_o} \right) + \frac{\partial G_F}{\partial t} - R_L \left(\frac{\partial N_p}{\partial t} \right) \end{aligned} \quad \dots (1)$$

For oil:

$$\nabla \cdot \left[\left(\frac{kh}{B\mu} \right)_o \nabla \Phi_o \right] = \frac{\partial}{\partial t} \left(\phi h \frac{S_o}{B_o} \right) + \frac{\partial N_p}{\partial t} \quad \dots (2)$$

For water:

$$\nabla \cdot \left[\left(\frac{kh}{B\mu} \right)_w \nabla \Phi_w \right] = \frac{\partial}{\partial t} \left(\phi h \frac{S_w}{B_w} \right) + \frac{\partial W}{\partial t} \quad \dots (3)$$

where $\nabla = i \frac{\partial}{\partial x} + j \frac{\partial}{\partial y}$, the nabla differential operator.

Equation (1) above is equivalent to the Muskat³ total gas balance. These equations state that the rate of influx of fluid into a specific region must be equal to the rate of accumulation plus the production of that fluid phase. In the case of equation (1), the additional terms

$$\frac{\partial}{\partial t} \left(\frac{\phi h R_L S_o}{B_o} \right), \nabla \cdot \left[R_L \left(\frac{kh}{B\mu} \right)_o \nabla \Phi_o \right], \text{ and } R_L \left(\frac{\partial N_p}{\partial t} \right)$$

are incorporated to account for the transfer of gas into and out of solution from the oil in the block and the oil entering or leaving the block, and it is easy to show that a solution of equation (1) in conjunction with the oil balance of equation (2) constitutes a conservation of total gas in the system. The velocity potentials are as follows:

$$\Phi_w = p + \rho_w gh + p_{cw}$$

$$\Phi_o = p + \rho_o gh + p_{co}$$

$$\Phi_g = p + \rho_g gh$$

The equations above are utilized later with:

$$S_w + S_o + S_g = 1 \quad \dots (4)$$

and

$$\frac{\partial}{\partial t} (S_w + S_o + S_g) = 0 \quad \dots (5)$$

to form a single pressure equation to be solved. The procedure will be to expand equations (1), (2), and (3) and take their sum to form a single differential equation with the dependent variable being pressure. Multiplying equation (1) by B_g and expanding gives:

$$\begin{aligned} B_g \nabla \cdot \left[\left(\frac{kh}{B\mu} \right)_g \nabla \Phi_g \right] &= \phi h \left[\frac{\partial S_g}{\partial t} - \frac{S_g}{B_g} \frac{\partial B_g}{\partial t} \right] \\ &- B_g R_L \left\{ \nabla \cdot \left[\left(\frac{kh}{B\mu} \right)_o \nabla \Phi_o \right] - \frac{\partial}{\partial t} \left(\frac{\phi h S_o}{B_o} \right) - \frac{\partial N_p}{\partial t} \right\} \\ &- B_g \phi h \left(\frac{S_o}{B_o} \right) \frac{\partial R_L}{\partial t} + B_g \frac{\partial G_F}{\partial t} + h S_g \frac{\partial \phi}{\partial t} \\ &+ B_g \nabla R_L \left(\frac{kh}{B\mu} \right)_o \nabla \Phi_o \end{aligned}$$

Since by equation (2)

$$\frac{\partial}{\partial t} \left(\phi h \frac{S_o}{B_o} \right) = \nabla \cdot \left[\left(\frac{kh}{B\mu} \right)_o \nabla \Phi_o \right] - \frac{\partial N_p}{\partial t}$$

this expanded equation can be simplified to the following:

$$\begin{aligned} B_g \nabla \cdot \left[\left(\frac{kh}{B\mu} \right)_g \nabla \Phi_g \right] &= \phi h \left[\frac{\partial S_g}{\partial t} - \frac{S_g}{B_g} \frac{\partial B_g}{\partial t} \right] \\ &- B_g \phi h \left(\frac{S_o}{B_o} \right) \frac{\partial R_L}{\partial t} + S_g h \frac{\partial \phi}{\partial t} \\ &+ B_g \nabla R_L \left(\frac{kh}{B\mu} \right)_o \nabla \Phi_o + B_g \frac{\partial G_F}{\partial t} \end{aligned} \quad \dots (6)$$

A similar procedure applied to the oil and water balance yields:

$$\begin{aligned} B_o \nabla \cdot \left[\left(\frac{kh}{B\mu} \right)_o \nabla \Phi_o \right] &= \phi h \left[\frac{\partial S_o}{\partial t} - \frac{S_o}{B_o} \frac{\partial B_o}{\partial t} \right] \\ &+ S_o \frac{h \partial \phi}{\partial t} + B_o \frac{\partial N_p}{\partial t} \end{aligned} \quad \dots (7)$$

$$\begin{aligned} B_w \nabla \cdot \left[\left(\frac{kh}{B\mu} \right)_w \nabla \Phi_w \right] &= \phi h \left[\frac{\partial S_w}{\partial t} - \frac{S_w}{B_w} \frac{\partial B_w}{\partial t} \right] \\ &+ S_w \frac{h \partial \phi}{\partial t} + B_w \frac{\partial N_p}{\partial t} \end{aligned} \quad \dots (8)$$

Now, summing equations (6), (7), and (8),

rearranging terms, simplifying with the results of equations (4) and (5), and expressing the volume factor changes as functions of pressure and temperature gives:

$$\begin{aligned}
 & B_g \nabla \cdot \left[\left(\frac{kh}{B\mu} \right)_g \nabla \Phi_g \right] + B_o \nabla \cdot \left[\left(\frac{kh}{B\mu} \right)_o \nabla \Phi_o \right] \\
 & - B_g \nabla R_L \left(\frac{kh}{B\mu} \right)_o \nabla \Phi_o + B_w \nabla \cdot \left[\left(\frac{kh}{B\mu} \right)_w \nabla \Phi_w \right] \\
 & - \left\{ B_g \frac{\partial G_F}{\partial t} + B_o \frac{\partial N}{\partial t} + B_w \frac{\partial N}{\partial t} \right\} + \\
 & \frac{\phi h \rho p}{\partial t} \left\{ \frac{S_g}{B_g} \frac{\partial B_g}{\partial p} + \frac{S_o}{B_o} \left[\frac{\partial B_o}{\partial p} + B_g \frac{\partial R_L}{\partial p} \right] + \frac{S_w}{B_w} \frac{\partial B_w}{\partial p} \right\} \\
 & + \frac{\phi h \partial T}{\partial t} \left\{ \frac{S_g}{B_g} \frac{\partial B_g}{\partial T} + \frac{S_o}{B_o} \left[\frac{\partial B_o}{\partial T} + B_g \frac{\partial R_L}{\partial T} \right] \right. \\
 & \left. + \frac{S_w}{B_w} \frac{\partial B_w}{\partial T} \right\} - \frac{h \partial \phi}{\partial t} = 0 \quad \dots (9)
 \end{aligned}$$

Equation (9) is a nonlinear partial differential equation describing the pressure and temperature distribution in a petroleum reservoir under conditions of the simultaneous flow of three fluid phases (oil, gas, and water). Since the various coefficients of this equation depend on pressure, temperature, and saturation, the equation cannot be solved by classical means. Therefore, finite difference techniques are used to obtain a solution.

The alternating direction implicit procedure of Peaceman and Rachford is used, with the exception that a time average of the pressure, temperature, and saturation dependent variables is employed instead of the ordinary backward time estimate of these terms. A general description of the procedure follows.

Basically, equation (9) can be put in the simple form:

$$\begin{aligned}
 & f_1(p, T) \nabla \cdot \left[\left(\frac{kh}{B\mu} \right)_g \nabla \Phi_g \right] + f_2(p, T) \nabla \cdot \left[\left(\frac{kh}{B\mu} \right)_o \nabla \Phi_o \right] \\
 & + f_3(p, T) \nabla \cdot \left[\left(\frac{kh}{B\mu} \right)_w \nabla \Phi_w \right] - g_1(p, T, S) + \phi h g_2(p, T, S) \frac{\partial p}{\partial t} \\
 & + \phi h g_3(p, T, S) \frac{\partial T}{\partial t} - \frac{h \partial \phi}{\partial t} = 0 \quad \dots (10)
 \end{aligned}$$

Adopting a normal orthogonal integration net of mesh size Δx , Δy , and utilizing the notation

$$\Delta x^2 (\Phi_o^{n+1})_{i,j} = \frac{\left[\left(\frac{kh}{B\mu} \right)_o^{n+\frac{1}{2}} \right]_{i+\frac{1}{2},j} (\Phi_o^{n+1})_{i+1,j} - (\Phi_o^{n+1})_{i,j}}{\Delta x}$$

$$- \frac{\left[\left(\frac{kh}{B\mu} \right)_o^{n+\frac{1}{2}} \right]_{i-\frac{1}{2},j} (\Phi_o^{n+1})_{i,j} - (\Phi_o^{n+1})_{i-1,j}}{\Delta x}$$

equation (10) is approximated with a difference equation of the type

$$\begin{aligned}
 & \left[f_1^{n+1}(p, T) \Delta x^2 (\Phi_g^{n+1})_{i,j} + f_1^{n+1}(p, T) \Delta y^2 (\Phi_g^n)_{i,j} \right] + \\
 & \left[f_2^{n+1}(p, T) \Delta x^2 (\Phi_o^{n+1})_{i,j} + f_2^{n+1}(p, T) \Delta y^2 (\Phi_o^n)_{i,j} \right] + \\
 & \left[f_3^{n+1}(p, T) \Delta x^2 (\Phi_w^{n+1})_{i,j} + f_3^{n+1}(p, T) \Delta y^2 (\Phi_w^n)_{i,j} \right] - \\
 & g_1(p, T, S) + \phi h g_2(p, T, S) \frac{(p_{i,j}^{n+1} - p_{i,j}^n)}{\Delta t} + \\
 & \phi h g_3(p, T, S) \frac{(T_{i,j}^{n+1} - T_{i,j}^n)}{\Delta t} - \frac{h \Delta \phi}{\Delta t} = 0 \quad \dots (11)
 \end{aligned}$$

where the ordinary derivatives immersed in the coefficient g_1 are evaluated by straightforward difference quotients. Equation (11) is said to be implicit in the x -direction since the y -direction difference quotients do not involve the unknown potentials (and hence pressures) at the time level $n+1$. Peaceman and Rachford outlined the alternating direction implicit procedure in detail. Briefly, it is as follows. Since, by assumption, the pressures in all three phases are equal, equation (11), when written for the point i, j , involves only three unknown pressures:

$$p_{i-1,j}^{n+1}, \quad p_{i,j}^{n+1}, \quad \text{and} \quad p_{i+1,j}^{n+1}$$

Hence, when equation (11) is written for each point of a row in the integration net (see Figure 2), a system of equations is obtained which are assumed linear over a time period Δt . This system of equations involves only a tri-diagonal coefficient matrix and therefore can be efficiently solved by straightforward elimination. The overall procedure is to solve equation (11) for each row in the integration net for one-half a time step ($\Delta t/2$), and then solve an equation like equation (11), except that it is written in the y -direction (that is, the time level indexes are reversed), for each column in the integration net for the remaining one-half time step. This alternating direction procedure has proved to be an efficient method of performing the numerical integration of a wide class of differential equations.

The coefficients of equation (11), however, depend on the unknown pressures as well as on the temperature and saturations; therefore, the procedure is a trial-and-error process. First an estimate of future pressures, temperatures, and saturations is made; then

the various coefficients are calculated and a trial solution of pressures is obtained. With the calculated pressures an explicit determination of saturation and temperature is made, and pressures, temperatures, and saturations are then compared with the previously made estimates. If agreement is not within a predetermined range, then an iteration is made. Otherwise the calculation proceeds to the next time step. When a trend is established, a simple linear extrapolation of pressures and saturations is used to estimate the future values. Special provisions are made when estimating saturations, pressures, and temperatures at a well point. Steam flow may occur in the reservoir as a part of the vapor phase. The phase relationship between water and steam is expressed in terms of steam quality, temperature, and pressure.

The overall trial-and-error process appears to converge rapidly and yields a practical solution to the problem. An overall material balance is performed after each time step to monitor the calculation. These material balance checks are usually accurate and indicate that at least the resulting solutions are obeying the law of mass conservation. In the above described three-phase flow, however, the water may be either liquid or vapor or at any quality between these two. The latent heat of vaporization is taken into account as a water phase flows from one cell to another and heat energy is transferred. A number of calculations were made to determine the significance of heat flow by conduction, and it was concluded (as it has been concluded by a number of authors) that it is of minor significance in most field problems and therefore was ignored. If the temperature is sufficiently high, and the pressure in a given cell or throughout the matrix is low, then water in the vapor phase may exist in this model.

DESCRIPTION OF USES

The numerical model herein described is two-dimensional, three-phase, and unsteady-state. The water phase may be liquid, vapor, or a combination of both. Changes in pore volume due to rock compressibility and thermal expansion are considered.

In the basic version the effect of temperature on permeability is not considered because of the limited data available in this area that would be generally applicable. However, input data provisions for these parameters were made available which, when coupled with one particular subroutine will allow for this change. This model has been used in the vertical configuration, both linearly and radially as shown in Figures 3 and 4 respectively. Flow may occur through the four faces separated by Δx or Δy dimensions but not through those separated by "thick" or "theta" dimensions of Figures 3 and 4. Gravity is fully effective so that denser fluids move structurally downward in relation to the lighter ones if both are subject to the same viscous forces.

Most uses for a thermal model result from some gross reservoir problem such as heavy oil, low pressure

energy level, etc. However, at this time, except for in situ combustion many of the solutions are found by studying and solving individual well problems (that is, drawdown, viscosity, and saturation changes primarily in the wellbore area). The uses stated below and those in which the model has been used to date have been vertical or cross sectional problems:

1. Well treating by in situ combustion process.
2. Thermal effects on water coning.
3. Steam injection.
4. Steam soak and/or hot water soak.

This model has been tested or used on all of the above processes and some of them are described in the following section.

DISCUSSION OF RESULTS

When evaluating in situ combustion processes it is necessary to calculate the resulting saturations and temperature after a cell or cells have been burned outside the model. The model does not now contain the stoichiometry necessary to make these determinations. Once this has been accomplished, the results may be placed into the model and it put into dynamic operation either to "idle," produce, or inject a fluid into the burned cell or cells or into adjacent cells. Allowing the model to "idle" (neither producing nor injecting) provides a method of observing the fluid redistribution. Immediate production or injection into the burned cells allows one to study the productivity or injectivity after the stimulation. Figure 5 displays what has been observed typically producing such a cell. After combustion the burned region must undergo a resaturation process before it can produce substantial quantities of oil if the drawdown is limited. In this case flowing bottom-hole pressure was held constant and the cells produced quantities of oil, gas (air), and water as dictated by the saturations and relative permeabilities. Even though the viscosity of this particular crude oil was very substantially affected by heat, the production of hot oil from the burned section was not very large for an extended period. All of the water production shown in Figure 5 is that resulting as a combustion product.

A schematic of the production and injection arrangement for a series of tests is shown in Figure 6. It represents a linear vertical section containing two wells which produce at constant flowing bottom-hole pressure. Thus the rate declines from 63 to 57 barrels of oil per day during the 1.15 years shown. The injection rate is held constant at 500 barrels of water per day at 400° C which is steam. However, it could as easily have been set to a percentage of reservoir withdrawals. Since the pressure in the injection cells is about 1,000 psia, this steam condenses upon entering the cell. Due to the volume and temperature it is transporting large amounts of heat energy to the matrix. Variations in permeability, coupled with the fact that the upper perforations are closer to the gas cap, account

for these perforations taking the majority of the steam. Figures 7 and 8 show the change in water saturation and temperature rise respectively. It may be noted that one of the injection cells has undergone a temperature increase of 94° C.

The final change in water saturations and the temperature rise shown for this series are given in Figures 9 and 10 respectively. The increase in water saturation has moved until there is a continuous increase from the injection cells almost to the producing cells. The temperature is continuing to increase in all injection cells and a nose or finger has developed and is moving toward the producing cells. In addition to normal pressure and saturation maps, this particular model displays temperature and steam quality maps. Although the results of the latter are not shown, the water in these cells has not begun to vaporize.

CONCLUSIONS

Numerical simulators describing fluid and heat flow are definitely useful in solving practical problems. Such models have been developed and are currently available as operational tools. Thermal techniques can be misapplied, however, and a simulation by numerical techniques can enable one to fully evaluate the method before committing the reservoir to it. Once burned, an alternate method cannot be implemented.

It is far less expensive to investigate recovery techniques by reservoir model than by field test, especially when many theories can be explored by computer for approximately the cost of one physical test or less.

NOMENCLATURE

- B = Formation volume factor, dimensionless
 G_F = Free gas produced
 h = Thickness
 k = Absolute permeability
 N_p = Oil produced
 p = Pressure
 R_L = Liberated gas-oil ratio = $R_{sj} - R_s$
 R_s = Solution gas-oil ratio
 S = Saturation
 Δt = Time interval
 W_p = Water produced
 ϕ = Porosity
 μ = Viscosity
 ρ = Density
 Φ = Potential, total

Subscripts, limits, operators

- i = Index of number of perforated intervals in a well
 i, j = Indices of block location in grid system
 o, g, w
 = Oil, gas, water

REFERENCES

1. Fagin, R. G. and Stewart, C. H.: "A New Approach to the Two-Dimensional Multiphase Reservoir Simulator," Trans. AIME (1966) Vol. 237, p. 175.
2. Peaceman, D. W. and Rachford, H. H., Jr.: "The Numerical Solution of Parabolic and Elliptic Differential Equations," Jour. Soc. Ind. Applied Math. (1955), 3, 28-41.
3. Muskat, Morris: Physical Principles of Oil Production, McGraw-Hill Book Co., New York (1949).

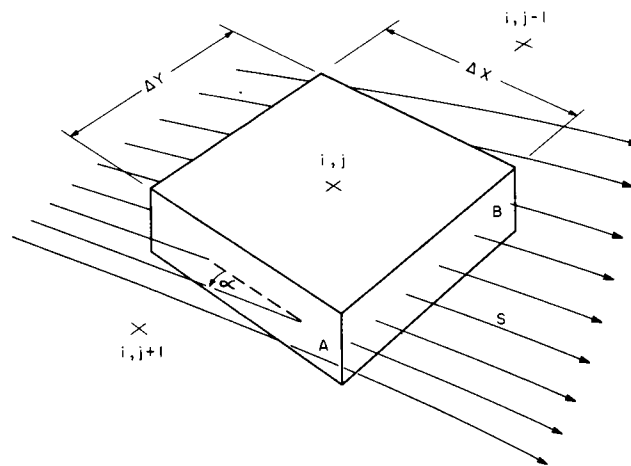


FIGURE 1 TYPICAL RESERVOIR ELEMENT

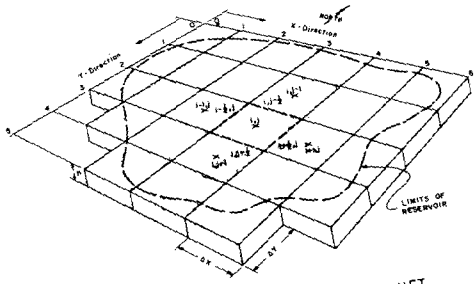


FIGURE 2 TYPICAL INTEGRATION NET

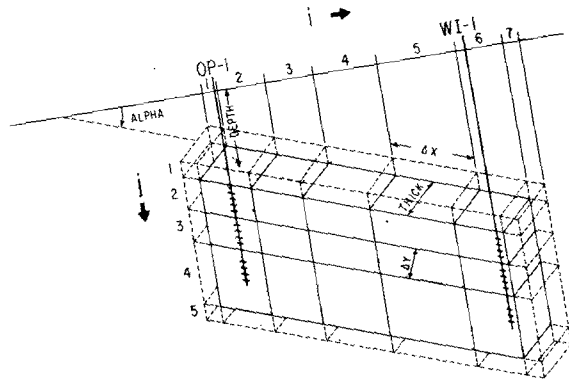


FIGURE 3 LINEAR CONFIGURATION

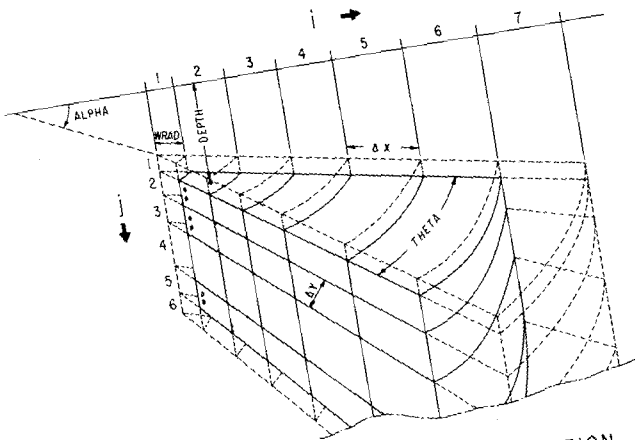


FIGURE 4 RADIAL CONFIGURATION

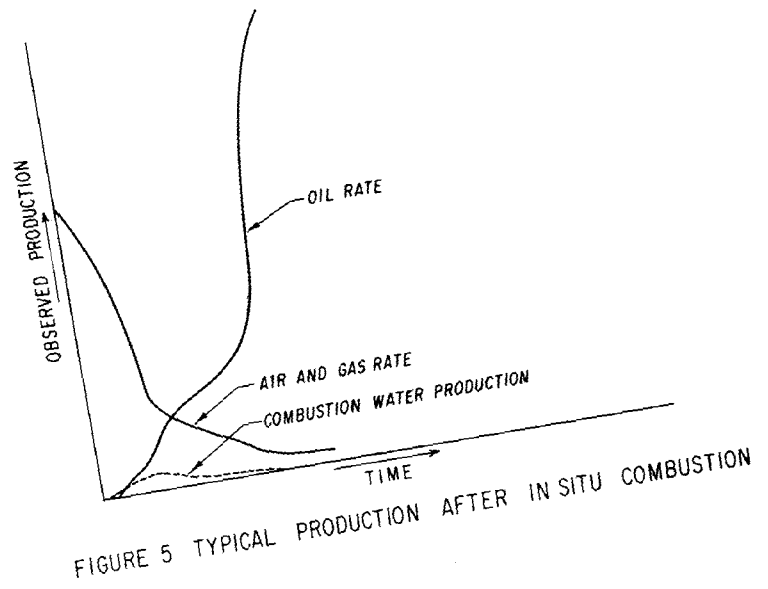
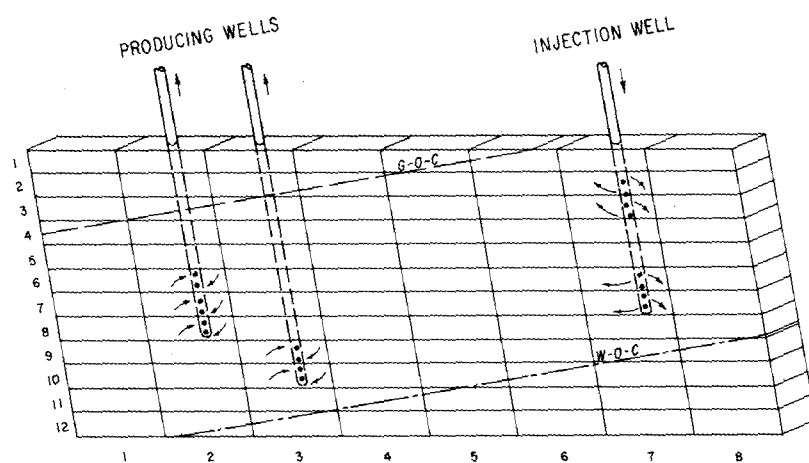


FIGURE 5 TYPICAL PRODUCTION AFTER IN SITU COMBUSTION



RES. TEMP. 99°C

FIGURE 6 SCHEMATIC OF PRODUCTION AND INJECTION

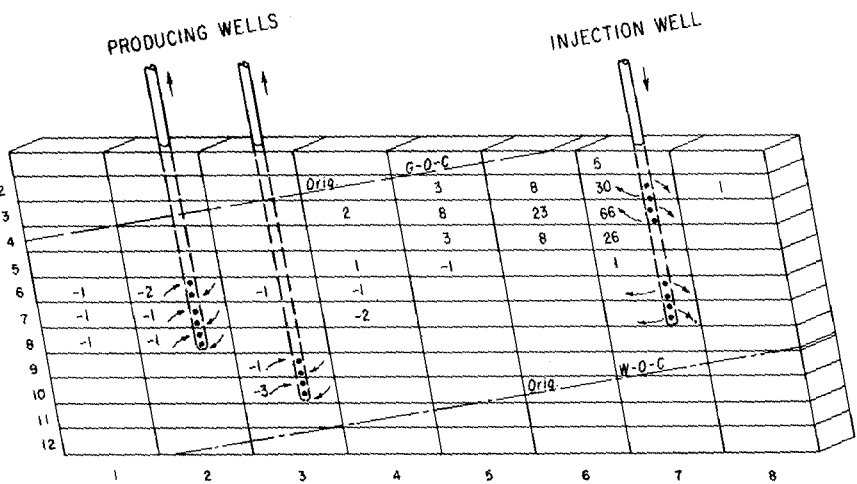


FIGURE 7 WATER SATURATION CHANGE - % @ 1966.325

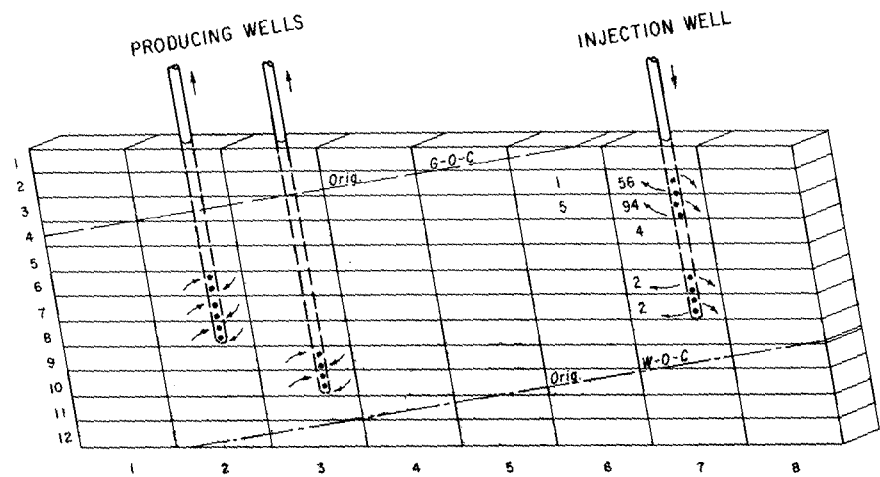


FIGURE 8 TEMPERATURE RISE - C° @ 1966.325

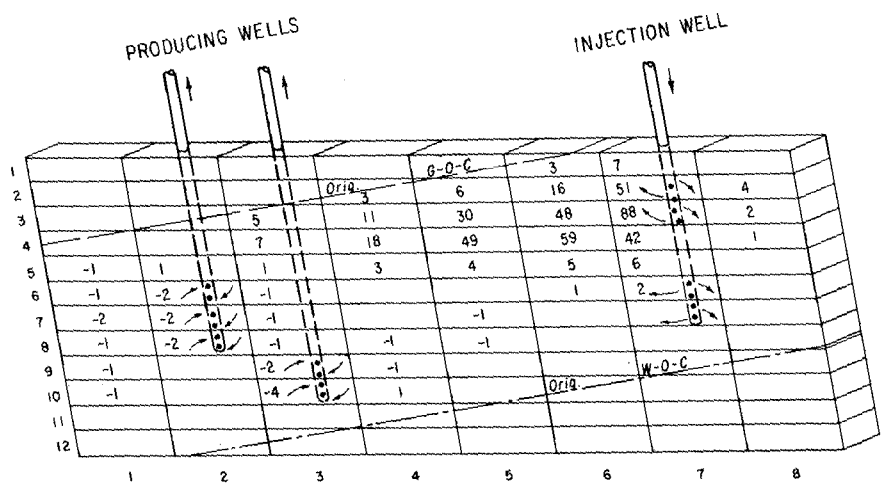


FIGURE 9 WATER SATURATION CHANGE - % @ 1966.900

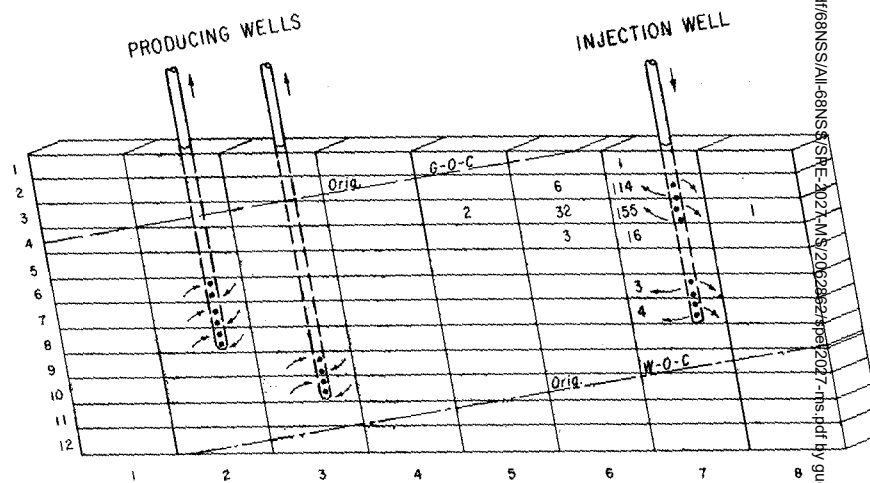


FIGURE 10 TEMPERATURE RISE - C° @ 1966.900